Atomic Micromanipulation with Magnetic Surface Traps

J. Reichel, W. Hänsel, and T. W. Hänsch
Max-Planck-Institut für Quantenoptik and Sektion Physik der Ludwig-Maximilians-Universität, Schellingstrasse 4, D-80799 München, Germany
(Received 6 July 1999)

We describe manipulation of neutral atoms using the magnetic field of microfabricated current-carrying conductors. It is shown how this method can be used to achieve adiabatic magnetic transport from one reservoir to another. In the first experimental realization of a microfabricated magnetic neutral-atom trap, efficient loading is achieved with a novel mirror-magneto-optic trap. A cloud of rubidium atoms is stored and compressed using the magnetic field of a "U"-shaped wire carrying a current of 2 A. An evaporation mechanism is demonstrated which removes hot atoms from the trap by collisions with the substrate surface.

PACS numbers: 32.80.Pj, 03.67.Lx, 03.75.–b, 39.90.+d

With the ground-breaking recent advances in the preparation of cold degenerate atomic ensembles [1], there is now a need for devices that can manipulate the atomic de Broglie waves in quantized states of external potentials in a controlled manner. This is true for atomic ensembles as well as for individual atoms. For instance, a single-mode matter waveguide would decisively enlarge the applicability of the coherent matter waves that are produced by atom lasers [2]. In cavity QED with cold atoms [3,4], the use of trapped atoms will lead to a new level of control over the atom-field interaction. The microscopic manipulation of atoms may also permit the realization of novel quantum gates, similar to those proposed for atoms in optical lattices [5]. In all these cases, the confining potential must be extremely steep to achieve a large mode spacing and a small ground-state size. Strong coupling of a trapped rubidium atom to the evanescent wave of a microsphere resonator, for example, would require a ground-state extension normal to the sphere on the order of $\lambda/2\pi \approx 124$ nm [6]. To achieve a $1/e$ ground-state diameter of this size in a harmonic magnetic potential, a field curvature of 55.7 kT/cm^2 is required.

Proposed magnetic microtraps and waveguides which replace the customary macroscopic field coils by a planar system of current-carrying conductors [7,8] or by a magnetized surface [9] hold promise for many new applications in this context. It has been pointed out [7] that, when a magnetic potential is created by a system of wires with characteristic size s and carrying a current I, the trapping field gradient and curvature, respectively, scale as I/s^2 and I/s^3 when s is decreased. Such "wire traps" can therefore provide very tightly confining potentials with much less power dissipation than "traditional" traps using macroscopic coils. First steps in this direction were taken with the realization of neutral-atom traps [10] and guides [11] that use thin, free-standing wires. When microfabricated conductors on a substrate surface are used for trapping, as demonstrated here for the first time, new possibilities open up that go beyond the mere production of steeper traps. Indeed, this approach enables the realization of new devices for atomic micromanipulation, such as the adiabatic "motor" which we describe. Moreover, the substrate enables higher current densities due to efficient heat removal, and also gives rise to new physical effects such as the surface-induced evaporation mechanism which we demonstrate.

The trapping field used in our experiment results from superposing the field of a single wire with an external bias field B_0 (Fig. 1). This configuration, which has previously been used in our laboratory to trap atoms with a free-standing wire [10], results in a line of zero field parallel to the wire at a distance $r_0 = \frac{\mu_0}{2\pi}\frac{I}{B_0}$. In the vicinity of this minimum, the field modulus varies approximately linearly with a gradient that is equal to that of the wire alone. In this way, a two-dimensional quadrupole potential is obtained which has a steepness of $|\nabla B|\,(r_0) = \frac{2\pi}{\mu_0}\frac{B_0^2}{I}$ at the trap center [12]. The trap depth is given by the magnitude of the bias field B_0.

To obtain a three-dimensional trap, a wire of length l is bent at both ends so that it forms either a "U" or a "Z" (Fig. 2). The stretches of wire parallel to y contribute a field component along x, which is not compensated by the bias field B_0, thereby closing the trap at its ends. They also determine the type of the potential minimum. In the "U" case, their contributions cancel at the origin and a quadrupole trap is formed

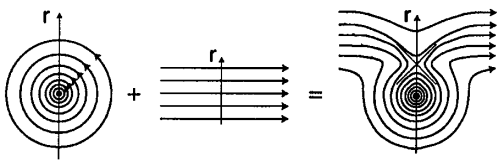

FIG. 1. Principle of the magnetic microtrap. A homogeneous bias field B_0 is superposed on the field of a microscopic current-carrying wire. The resulting field has a minimum along the wire axis.

 0031-9007/99/83(17)/3398(4)$15.00

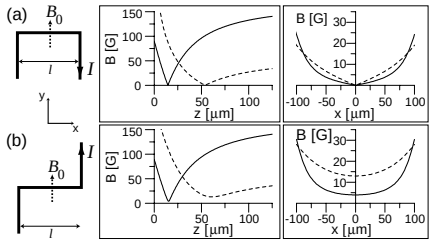

FIG. 2. Wire layout for a (a) quadrupole and (b) Ioffe-Pritchard trap. Magnetic potentials generated by these arrangements for $l = 250\ \mu$m and $I = 2$ A. The bias field along y is $B_0 = 54$ G (dashed lines) and 162 G (solid lines). The potentials shown in the figure were obtained by simple Biot-Savart type calculations, including a wire width of 50 μm.

[Fig. 2(a)]. In the "Z" configuration, the contributions add, and the trap is of the Ioffe-Pritchard type [Fig. 2(b)]. With our current microfabrication process (see below), we have obtained sustainable currents of more than 2 A through wires of approximately 2 cm length with a rectangular cross section 3 to 4 μm high and 50 μm wide. With this current and a bias field strength of 162 G, a transverse field gradient of 5.6 T/cm is obtained in the "U" configuration. In the "Z" configuration with a length $l = 250\ \mu$m, the transverse curvature is 57.4 kT/cm^2, leading to a level spacing (in the harmonic approximation) of 30.4 kHz for ^{87}Rb atoms in the $F = 2, m = 2$ ground state, and to a ground-state size of 123 nm ($1/e$ diameter). This is small enough to provide efficient coupling of a trapped atom to the evanescent field of a microsphere resonator and also implies the Lamb-Dicke regime with respect to the rubium D_2 line.

Starting from these basic configurations, more complex potentials can be constructed, such as the atomic motor which is shown in Fig. 3. In this device, the Ioffe-Pritchard-type potential of Fig. 2 is modulated by the currents of the two undulating wires labeled I_{M1} and I_{M2}. In this way, a chain of separated minima is obtained which

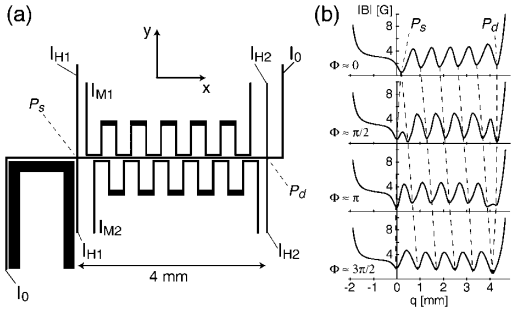

FIG. 3. (a) Wire layout for the "atomic motor." (b) Magnetic potential produced by this layout with a constant field $\vec{B}_0 = 3$ G $\vec{e}_x + 16$ G $\vec{e}_y$ and the following currents: $I_0 = 1.5$ A, $I_{M1} = 0.8$ A$\cos\phi$, $I_{M2} = 0.8$ A$\sin\phi$, $I_{H1} = -0.17$ A $+ 0.15$ A$\cos\phi$, $I_{H2} = -0.25$ A $+ 0.18$ A$\sin\phi$. The coordinate q follows the path of transverse (x-y plane) minimum for each value of the longitudinal x coordinate.

can be moved along the x axis by varying the currents I_{M1} and I_{M2}. The realization shown in Fig. 3 has two additional, stationary trapping minima, P_s and P_d, which are generated by the currents I_{H1} and I_{H2}. When phase-shifted alternating currents are applied as specified in the figure caption, moving minima separate off the "source" trap P_s and travel continuously to the right where they unite with the "destination" trap P_d. This process can be used to replenish the reservoir P_d. To illustrate this mechanism, Fig. 3(b) shows four phases of the time-varying potential. In this example, the field curvature in the minima is on the order of 1 T/cm^2 along its weakest axis—which is the direction of transport—and more than a factor of 20 larger in the plane orthogonal to it. Note that the potential minima are nonzero for all times, which is important to avoid Majorana losses. Phase-space density can be increased if evaporative cooling occurs during the transport. Furthermore, the same device could be used to position individual atoms inside an optical cavity. Note also that the distance between P_s and P_d can be increased, so that atoms can be transported over truly macroscopic distances while remaining tightly confined.

Given such prospects, it is understandable that considerable effort is being put into the development of electromagnetic microtraps [10,11,13]. Although, however, microfabricated electromagnetic mirrors have been demonstrated [13,14], several major experimental obstacles prevented the realization of a microfabricated atom trap up until now. In particular, loading of the microtrap from a magneto-optic trap (MOT) is hindered by the microtrap's small volume and by the proximity of the substrate, which is incompatible with the laser beam arrangement of a standard six-beam MOT. Our solution introduces the *mirror-MOT*, a modified version of the magneto-optical trap which works in proximity of a reflecting surface.

The mirror-MOT [Fig. 4(a)] is a variant of the standard magneto-optical trap which cools and traps atoms close to a surface. Unlike other surface MOTs [15,16], it does not require a transparent material, but rather makes use of a mirror surface. It uses only four instead of the usual six laser beams, two of which are reflected off the mirror surface, with the polarizations and magnetic field orientation shown in Fig. 4(a). In this way, the usual

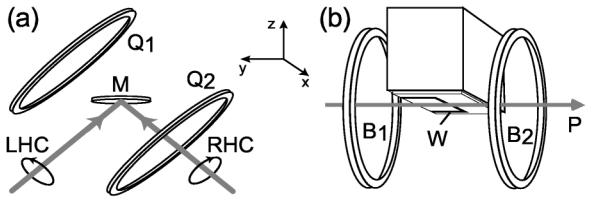

FIG. 4. (a) Schematic of the mirror-MOT. M: mirror, Q_1, Q_2: quadrupole coils. (b) Setup of the experiment. W: microfabricated wire, B_1, B_2: bias coils, P: probe beam. (MOT beams and coils not shown.)

MOT geometry is realized in the half space delimited by the substrate. The MOT typically contains 5×10^6 atoms if the distance from the surface is larger than 1 mm. For smaller distances, the decay time constant decreases, leading to a smaller steady-state number of trapped atoms. We therefore load the trap far from the surface and then shift it by displacing the quadrupole center.

Our substrates are manufactured using *thin-film hybrid technology*. This standard procedure from microelectronics packaging combines photolithography and electroplating and is well adapted to high current densities. (A very similar process has been described in [13].) The most frequently used materials are aluminum oxide for the substrate and gold for the conductors. Other substrate materials such as sapphire or diamond and other metals are also available. The electroplating results in a wire thickness of 3 to 6 μm; the minimum wire width is of the same order.

Our first demonstration of an integrated microtrap uses a quadrupole potential of the type of Fig. 2(a). It employs a U-shaped gold wire which is realized as a simple hybrid circuit on an aluminum-oxide ceramic substrate. The wire has a rectangular cross section 300 μm wide and 3.8 μm high, and has a length l of 1.5 mm. To combine it with the mirror-MOT, the substrate was coated with a sputtered silver layer (200 nm thickness) on top of an isolating photoresist (thickness on the order of 1 μm). The geometry of the experiment is shown in Fig. 4(b). The substrate is mounted upside down on a copper block hanging in a UHV glass cell, which is pumped by a 25 l/s ion pump to a pressure in the lower 10^{-9} mbar range. Outside the cell, a pair of coils generates the bias field.

A typical experiment is carried out as follows: During 4 s, ^{87}Rb atoms are collected from the background vapor in the mirror-MOT using the external quadrupole coils. After loading, the cold atom cloud is shifted from its initial position at $z \sim -2.2$ mm (below the substrate) to $z \sim -1.1$ mm by imbalancing the currents in the quadrupole coils. Next, the quadrupole field of the MOT coils is switched off and replaced by the magnetic field of the microtrap, using a wire current $I = 2$ A and a bias field $B_0 = 1.8$ G along y. The atoms remain magneto-optically trapped because the quadrupole field axes of the MOT coils coincide with those of the microtrap. In this way, the MOT is shifted to the exact location of the microtrap, making the alignment of the quadrupole coils uncritical. The cloud is subsequently compressed and shifted by reducing the wire current, increasing the trapping laser detuning, and lowering the intensity of the repumping light, then cooled in optical molasses and optically pumped to the $5S, F = 2, m_F = 2$ state. This sequence results in an elliptical cloud at $z \sim -0.3$ mm, containing on average 4×10^6 atoms at a temperature of 30 μK. At this point, all lasers are shut off and the magnetic microtrap is switched on with $I = 2$ A and $B_0 = 9$ G.

Figure 5 shows an absorption image of the atom cloud after 100 ms of magnetic trapping, taken 200 μs after the trap was switched off. The horizontal and vertical cuts through the center of the cloud clearly show the non-Gaussian shape of the density distribution, which is due to the particular form of the microtrap potential [cf. Fig. 2(a)]. The number of atoms N_{at}, as determined by integration over the absorption image, is $N_{\mathrm{at}} = 2.3 \times 10^6$. Indeed, transfer efficiencies of about 50% are typical in this experiment. We have recorded N_{at} as a function of the trapping time t by repeating the cycle for trapping times up to 2 s and find that $N_{\mathrm{at}}(t)$ is well fitted by a simple exponential decay function with a decay time constant that varies between 700 ms and 1200 ms, depending on the Rb background pressure.

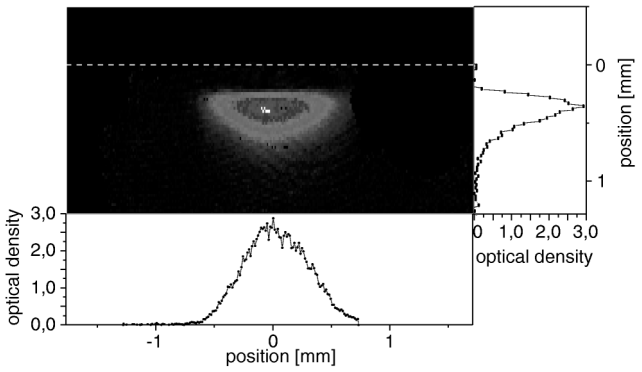

FIG. 5. Absorption image after 100 ms of magnetic trapping in the potential created by a U-shaped wire of 300 μm width carrying a current $I = 2$ A and a bias field $B_0 = 9$ G. The image was taken 200 μs after the magnetic trap was switched off. The position of the substrate surface is indicated by the dashed line.

When the bias field B_0 is increased while the wire current I is kept constant, the transverse gradient at the trap center increases with B_0 while the trap center moves closer to the surface. Figure 6 shows the position of the trap center as a function of B_0 for a constant wire current of $I = 2$ A. The squares are experimental values obtained from absorption images. The solid line is the theoretical position of the magnetic field minimum obtained from a Biot-Savart calculation of the wire and

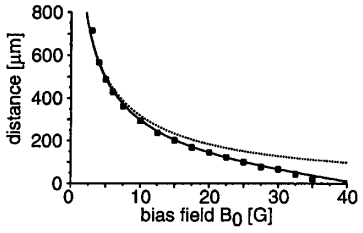

FIG. 6. Distance between the cloud center and the surface as a function of the bias field strength B_0. The wire current is kept constant at $I = 2$ A. Circles are experimental values obtained from absorption images; the solid line is the calculated position of the potential minimum for a wire of 300 μm width. For comparison, the dashed line gives the theoretical position for an infinitely thin wire.

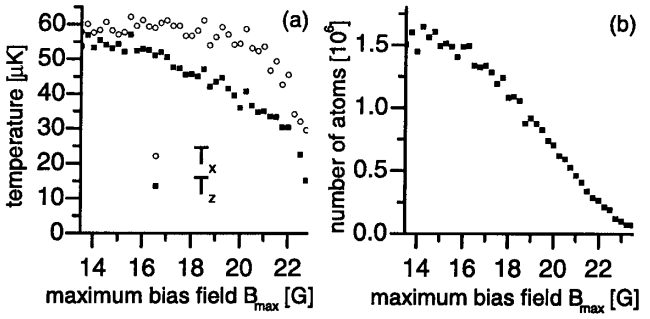

FIG. 7. Surface-induced evaporation. (a) Temperature of remaining atoms after shifting the cloud towards the surface by increasing B_0 up to $B_{\max}$, then shifting it back to a constant measurement position. (b) Number of atoms remaining in the trap after the shifting sequence.

bias field, including the finite width of the wire. For comparison, the dashed line indicates the position for an infinitely thin wire.

We have used this precise control of the trap position to selectively remove hot atoms from the trap. While the wire current is kept constant at 1.6 A, the bias field is ramped up to a final value $B_{\max}$ within 100 ms. The trap is shifted back 2 ms later, within another 100 ms, to a distance of $z = 300\ \mu$m from the surface ($I = 2$ A, $B_0 = 9$ G), where the trap parameters can be measured as a function of $B_{\max}$ under identical conditions. Atoms with an energy in the z direction in excess of the potential at the surface, μB_s, are removed from the trap by collisions with the surface. Elastic collisions between the remaining atoms subsequently reduce the temperature along all trap axes [17]. Figure 7(a) shows how the final temperatures in the x and z directions decrease for increasing $B_{\max}$. The decrease in the number of remaining atoms [Fig. 7(b)] is only partly due to the surface-induced evaporation. In the quadrupole trap, the compression of the trap also results in an increased loss rate due to Majorana spin flips, which is particularly pronounced in our trap because the gradient along the x direction decreases for large $B_{\max}$, resulting in a line of nearly vanishing magnetic field. Nevertheless, phase-space density increased in this experiment by more than a factor of 2. No attempt was made to optimize this gain factor; surface-induced evaporation will be studied in more detail in a future surface trap of the Ioffe-Pritchard type (cf. Fig. 2), where Majorana losses are suppressed.

We are currently testing substrates with more complex conductor structures and wire widths down to 20 μm. It should be noted that the trap-surface distance in these potentials is on the order of 20 μm from the surface, more than an order of magnitude above the distance at which interaction with the surface is expected to cause any measurable heating of the trapped atoms [18]. Traps with level spacings above the single-photon recoil energy, implementation of the atomic motor, and atom-optical devices such as beam splitters are feasible with these substrates.

We thank M. Kaleja, G. Olbrich, and P. Russer (Institut für Hochfrequenztechnik, Technische Universität München), M. Stuke (Max-Planck-Institut für Biophysikalische Chemie), and the Fraunhofer Institut für Festkörpertechnologie for providing us with test substrates, and M. Quintenz and M. Levenson for technological advice.

[1] For a recent review, see W. Ketterle, D. S. Durfee, and D. M. Stamper-Kurn, in Making, Probing and Understanding Bose-Einstein Condensates, Proceedings of the International School of Physics "Enrico Fermi," edited by M. Inguscio, S. Stringari, and C. Wieman [cond-mat/9904034 (1999)].
[2] M.-O. Mewes *et al.*, Phys. Rev. Lett. **78**, 582 (1997).
[3] C. Hood, M. Chapman, T. Lynn, and H. Kimble, Phys. Rev. Lett. **80**, 4157 (1998).
[4] P. Münstermann *et al.*, Phys. Rev. Lett. **82**, 3791 (1999).
[5] D. Jaksch *et al.*, Phys. Rev. Lett. **81**, 3108 (1998).
[6] F. Treussart *et al.*, Opt. Lett. **19**, 1651 (1994).
[7] J. D. Weinstein and K. G. Libbrecht, Phys. Rev. A **52**, 4004 (1995).
[8] J. H. Thywissen *et al.*, Eur. Phys. J. D (to be published).
[9] E. A. Hinds, M. G. Boshier, and I. G. Hughes, Phys. Rev. Lett. **80**, 645 (1998).
[10] J. Fortagh, A. Grossmann, C. Zimmermann, and T. W. Hänsch, Phys. Rev. Lett. **81**, 5310 (1998).
[11] J. Denschlag, D. Cassettari, and J. Schmiedmayer, Phys. Rev. Lett. **82**, 2014 (1999).
[12] For a long wire of width w and zero height, the magnetic field is $|B|(z) = \frac{\mu_0}{\pi}\frac{I}{w}\,\mathrm{arccot}(2z/w)$, where z is the distance from the wire. The modulus of the field gradient is $|\nabla B|(z) = \frac{\mu_0 I}{2\pi}\frac{1}{z^2+(w/2)^2}$.
[13] M. Drndić *et al.*, Appl. Phys. Lett. **72**, 2906 (1998).
[14] D. C. Lau *et al.*, Eur. Phys. J. D **5**, 193 (1999).
[15] Y. B. Ovchinnikov, I. Manek, and R. Grimm, Phys. Rev. Lett. **79**, 2225 (1997).
[16] T. Pfau and J. Mlynek, OSA Trends in Optics and Photonics **7**, 33 (1997).
[17] Because of decreasing density, thermalization during the back-shifting process is not complete. The change in trap aspect ratio during shifting therefore leads to a difference between transverse and longitudinal temperature.
[18] C. Henkel and M. Wilkens, quant-ph/9902009, 1999.